Earthquakes and Structures, *Vol. 19, No. 2 (2020) 103-117*
DOI: https://doi.org/10.12989/eas.2020.19.2.103

Foundation size effect on the efficiency of seismic base isolation using a layer of stone pebbles

Ivan Banović, Jure Radnić and Nikola Grgić*

University of Split, Faculty of Civil Engineering, Architecture and Geodesy, Matice hrvatske 15, 21000 Split, Republic of Croatia

(Received January 6, 2020, Revised June 2, 2020, Accepted August 6, 2020)

Abstract. The effect of the foundation size on the efficiency of seismic base isolation using a layer of stone pebbles is experimentally investigated. Four scaled models of buildings with different stiffnesses (from very stiff to soft) were tested, each with the so-called small and large foundation, and exposed to four different accelerograms (different predominant periods and durations). Tests were conducted so that the strains in the model remained elastic and afterwards the models were tested until collapse. Each model was tested for the case of the foundation being supported on a rigid base and on an aseismic layer. Compared to the smaller foundation, the larger foundation results in a reduced rocking effect, higher earthquake forces and lower bearing capacity of the tested models, with respectable efficiency (reduced strain/stress, displacement and increase of the ultimate bearing capacity of the model) for the considered seismic base isolation compared to the foundation on a rigid base.

Keywords: seismic base isolation; pebble layer; foundation size effect; shake-table study

1. Introduction

The application of seismic base isolation by various aseismic devices is becoming increasingly widespread. Unfortunately, some deficiencies (cost, complexity, durability, maintenance during building lifetime, etc.) are the reason why such seismic isolation is not yet widely used. According to Tsang (2009), in the past century, earthquakes have killed an average of over 20,000 people a year throughout the world, with 90% of fatalities occurring in developing countries. This fact indicates that low-cost and low-tech seismic base isolation is necessary. In recent years, simple solutions for seismic base isolation, suitable for less developed countries and simple structures, have been intensively explored. Such solutions, with sufficient efficiency and reliability, should be significantly more rational and easier to apply than the above aseismic devices.

The application of seismic base isolation using natural materials has been utilized throughout history (Przewłócki *et al*. 2005 and Carpani 2017). Historically, builders used layers of gravel, stone, and wood (multi-layered timber grillage) for the seismic base isolation of various buildings and bridges (Kulukčija *et al.* 2009, Kulukčija and Humo 2009). J.A. Calantarients, a medical doctor from England, at the beginning of 20th century proposed separation of the building from its foundation with a layer of sand or talk, as an earthquake resistant design approach (Naeim and Kelly 1999). Modern builders, guided by the experience of their predecessors, tend to find low-cost seismic base isolation. The development of such isolation goes in several directions, using different materials below the foundation including, sand, gravel, stone pebbles, rubber-soil mixtures (RSM), geofoam, and geosynthetics. All of these materials have the same purpose, namely, that seismic energy is dissipated before it transmits into the structure. Some of the most important studies are briefly outlined below.

New experimental and numerical studies on the use of sand and gravel for the seismic base isolation of buildings are increasing. Tehrani and Hasani (1996) performed an experimental study to evaluate the performance of sand and lightweight expanded clay for the seismic base isolation of buildings in Iran. Banović *et al.* (2018a) and Radnić *et al*. (2015) also proved by a shake-table study that layer of limestone sand can serve as a base isolation material. Patil *et al.* (2016) and Anastasopoulos *et al.* (2012) experimentally investigated the performance of river sand for seismic base isolation, while Zhao *et al.* (2016) numerically simulated a gravel isolation layer using a discrete element method. Seismic isolation using gravel has appeared in modern applications in the construction of the Rio-Antirion Bridge in Greece (Pecker *et al.* 2001), Vasco de Gama Bridge in Portugal (Pecker 2003) and the Izmit Bay Bridge in Turkey (Steenfelt *et al.* 2015).

Since it was first proposed by Tsang (2008), the concept of geotechnical seismic isolation (GSI) using a rubber-soil mixture (RMS) around the foundations of structures for absorbing seismic energy has attracted significant research interest. The effectiveness of the GSI system is analysed through numerical (Xiao *et al*. 2004, Mavronicola *et al.* 2010, Tsang *et al.* 2012, Panjamani *et al.* 2015, Bandyopadhyay *et al.* 2015, Brunet *et al.* 2016, Forcellini 2017, Tsiavos *et al.* 2019, Tsang and Pitilakis 2019) and experimental (Xiong and Li 2013, Xiong *et al.* 2014) studies. Other GSI research efforts are on soil replacement by geofoam (Murillo *et al.* 2009, Azinović *et al.* 2014, Azinović *et al.* 2016, Koren and Kilar 2016, Hadad *et al.* 2017, Karatzia *et al.* 2017, Azzam *et al.* 2018). The

*Corresponding author, Ph.D. Assistant Professor
E-mail: nikola.grgic@gradst.hr

http://www.techno-press.com/journals/was&subpage=7
ISSN: 2092-7614 (Print), 2092-7622 (Online)

application of smooth synthetic liners and geomembranes/geotextiles for dissipating seismic energy through sliding has also been proposed (Doudoumis *et al.* 2002, Yegian and Catan 2004, Yegian and Kadakal 2004, Nanda *et al.* 2012a, Nanda *et al*. 2012b, Kalpakci *et al.* 2018). The concept of rocking isolation as seismic protection strategy is studied by many researchers (Makris 2014, Chung *et al.* 2019, Feng *et al*. 2018, Wang *et al.* 2018).

Banović *et al.* (2018b, 2019) experimentally investigated the effectiveness of seismic base isolation using a layer of natural stone pebbles. First, a shake-table study on the efficiency of seismic base isolation using natural stone pebbles was performed (Banović *et al.* 2018b), with very encouraging research results. The models of stiff and medium-stiff buildings (a free-standing steel column with a concrete foundation and mass at the column top) were tested. Case studies were conducted on a model founded on the rigid base and on different layers of pebbles. Four different horizontal accelerograms were applied. The strains/stresses of the tested models remained in the elastic region. The results of the study showed that a layer of pebbles can significantly reduce the peak acceleration and strains/stresses of the model, with acceptable displacements.

After the very encouraging research results of the first study (Banović *et al.* 2018b), Banović *et al.* (2019) experimentally investigated the optimum properties of an aseismic stone pebble layer (the layer thickness, the fraction of pebbles, the pebble compaction, the pebble moisture, the vertical contact stress below the foundation, and the effect of repeated excitations).

This paper presents the results of further research related to the possibility of applying seismic base isolation using a layer of stone pebbles below the foundation, as previously shown in Banović *et al.* (2018b, 2019). The effect of the foundation size (ground plan dimensions), i.e., the foundation rotational stiffness, on the efficiency of the seismic isolation was investigated. The results of the tests are compared for two ground plan dimensions (stiffness) of the foundation, namely, the so-called small foundation (SF) and so-called large foundation (LF). Experimental tests on scaled models of buildings with four different stiffnesses (period of free oscillation) were performed. Increasing the rotational stiffness of the foundation eliminates the beneficial effect of rocking and therefore reduces the efficiency of seismic isolation. However, it was concluded that even in the case of a building where very low foundation rotation is possible, considered seismic isolation still exhibits considerable efficiency for low-rise very stiff and stiff buildings based on stiff soil.

2. Considered building models with foundation

The considered building models (M_1, M_2, M_3, and M_4) of different stiffnesses (periods of free oscillation T) with two types of foundations (SF and LF) are shown in Fig. 1. SF denotes a small foundation with dimensions of 0.7 x 0.5 x 0.3 m (m=260 kg), and LF denotes a large foundation with dimensions of 1.2 x 0.7 x 0.3 m (m=630 kg). Thus, the foundations (concrete with cube strength 46 MPa) are of equal height and different layout dimensions. The smaller foundation represents real buildings with a high rocking effect, while the large foundation represents those with a low rocking effect. The building models (Banović *et al*. 2018b) are free-standing steel columns (steel S355) with a concrete block (cube strength 46 MPa) of mass m=1000 kg at the column top. It should be noted that the complete oscillating mass is a sum of masses (block, column and foundation). Further, the structural response in the case of earthquake is governed by oscillating mass, column's stiffness, soil-structure-interaction and the stiffness and capacity of the column-foundation joint connection.

Models M_1 and M_2 have a column height of 1.02 m and models M_3 and M_4 have a column height of 2.02 m. The square hollow cross sections of the columns are different for the M_1-M_4 models, according to Fig. 1. Building models included in research represent a very wide stiffness range of potential buildings for possible application of this seismic isolation concept: M_1 – very stiff structure (T=0.05 s), M_2 – stiff structure (T=0.30 s), M_3 – medium-stiff structure (T=0.60 s) and M_4 – soft structure (T=1.40 s). Vibration period of models are calculated for linear system, without foundation and with rigid column-foundation joint connection. Vibration periods are verified on shake-table and are valid for rigid base case.

All samples were first tested for the case where the foundation is supported on a rigid base (allowing the foundation lifting, while the horizontal displacement of the foundation in relation to the shake-table is prevented). Fig. 1f reveals how the lifting was enabled and horizontal displacement prevented, simultaneously. Also, compared to the fixed base support case, this support case produces usually lower seismic forces on the model, which gives more conservative seismic base isolation efficiency.

After that, models were tested with the foundation on a pebble layer with the following characteristics: thickness h_p=0.3 m, fraction Φ_b=16-32 mm, compaction MS=30 MPa and humidity v=10%, all analogous to the study in Banović *et al*. (2019). For the models based on pebble layer, sliding between the foundation and the stone pebbles in not prevented.

First part of the study was performed for one-time base acceleration so that the strains in the model remained elastic ($a_{g,\,max}$=0.3 g for M_1 and M_2 and with $a_{g,\,max}$=0.2 g for M_3 and M_4), and afterwards for the most unfavourable accelerogram the models were tested until collapse.

3. Base accelerations

Adopted base accelerations are presented in Fig. 2 (Banović *et al.* 2018b, 2019). The artificial accelerogram (AA) and accelerogram Petrovac (AP) (Ambraseys *et al.* 2001) represent long-lasting earthquakes with long predominant periods, while Ston (AS) and Banja Luka (ABL) (Ambraseys *et al.* 2001) accelerograms represent short-duration earthquakes with short predominant periods (impact earthquakes). The AA was created to match the elastic response spectrum according to EC 8 (2004) for

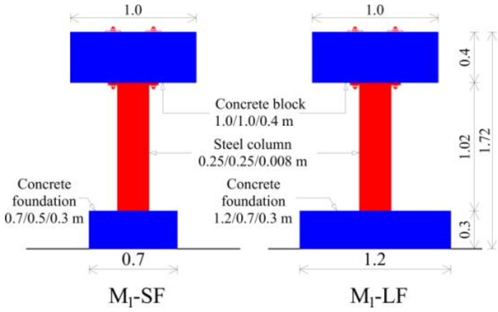

(a) Model M_1 (T = 0.05 s)

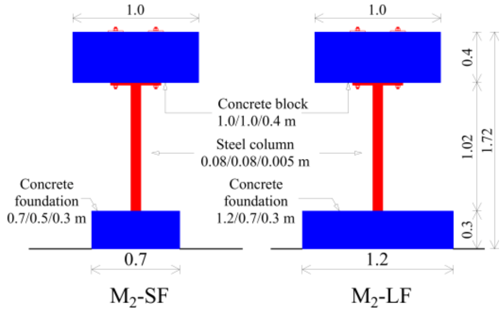

(b) Model M_2 (T = 0.30 s)

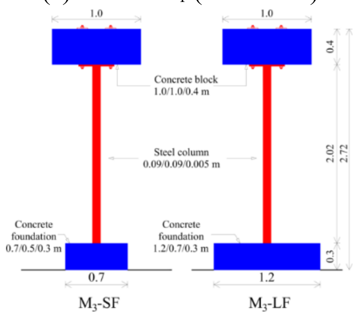

(c) Model M_3 (T = 0.60 s)

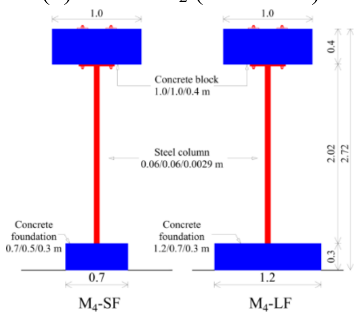

(d) Model M_4 (T = 1.40 s)

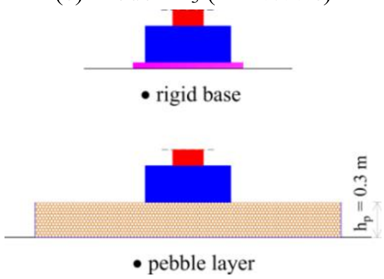

(e) Foundation support variants

(f) Foundation on rigid base: prevented horizontal displacement and enabled uplifting

Fig. 1 Considered building models

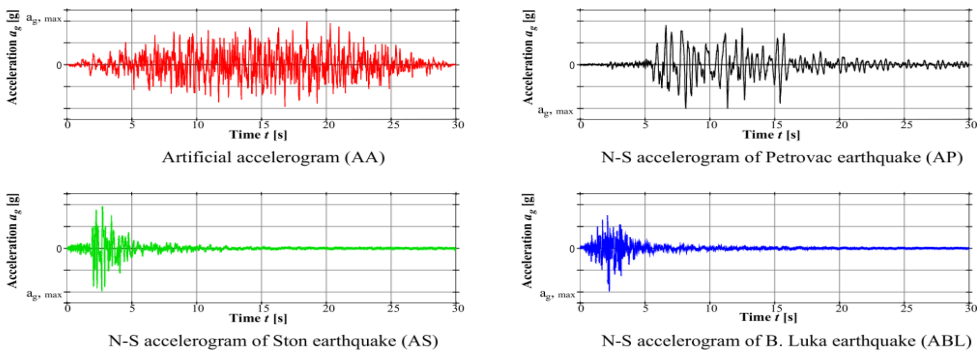

(a) Adopted horizontal base excitations

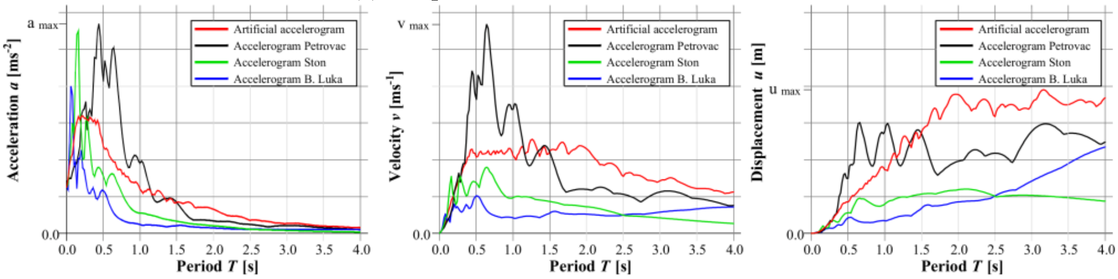

Spectral acceleration Spectral velocity Spectral displacement

(b) Elastic response spectra of adopted excitations

Fig. 2 Basic information on applied base excitations (Banović *et al.* 2018b, 2019)

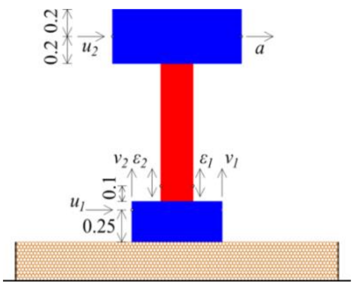

Fig. 3 Measured quantities

earthquake type 1 and soil type A. The AA and AP generate large displacements of the structure and bring high seismic energy with a strong bending effect, while AS and ABL have a more pronounced shear force effect.

4. Measured quantities and instrumentation

The following quantities were measured on each tested model (Fig. 3): the horizontal acceleration of the mass centre at the column top a, horizontal displacements u_1 (foundation top) and u_2 (mass centre at the column top), vertical displacements of the foundation v_1 (at the right edge) and v_2 (at the left edge), and vertical strains on the bottom of the steel column ε_1 (at the right side) and ε_2 (at the left side).

The uniaxial shake-table from the University of Split, Faculty of Civil Engineering, Architecture and Geodesy (Croatia) was used for model testing. A Quantum-x mx 840A (Hottinger Baldwin Messtechnik-HBM) high-speed data acquisition system was used for data collection and processing. The strains were measured using strain gauges, type 6/120 LY11 (HBM). A piezo-electric low-frequency accelerometer type 4610 (MS) measured the accelerations, and the displacements were measured using analogue displacement sensors, type PB-25-S10-N0S-10C (Uni Measure). The adopted sampling rate during the tests was 200 Hz. For test monitoring, a video camera (Canon EOS M5) was used.

5. Small-scale models

It is well known that a reduced model 1: n of a real structure (prototype), where n is the factor of its reduction, cannot fully describe the actual behaviour of the real structure in an earthquake. The inconsistencies increase as the levels of reduction and nonlinearities in the structure increase. Reduced models can be reliable when investigating the relative effect of a parameter on the behaviour of the actual structure, i.e., when performing a parametric analysis. Caution should be present when assessing the behaviour, local effects and degree of safety of a real structure based on reduced model testing.

A brief theoretical overview of the expected differences in the test results with different foundation sizes is discussed below. As the larger foundation is 1.2 m long and 0.7 m wide and the smaller foundation is 0.7 m long and 0.5 m wide, the ratio of the area, resistance moment and inertia torque of the larger to smaller foundations are 1.71, 4.11 and 7.05, respectively. Therefore, a larger foundation will have significantly smaller rotation angles. The consequence is that less of a rocking effect is observed, i.e., less influence of the nonlinearity on the contact of foundation and substrate. Due to the larger surface area and lower contact stresses, it is possible that the horizontal displacements of the larger foundation relative to the base may be larger than those of the small foundation. It is expected that the smaller effect of rocking on a larger foundation will be present for the case of a rigid base, as well as for the case of the foundation support being on a layer of stone pebbles.

Smaller dimensions of the foundation result in a lower structural stiffness, higher foundation rocking effect and smaller earthquake forces in the structure, which is convenient. However, in such cases, the collapse of the structure can often occur due to overturning, without exhausting the load-bearing capacity of the structure. The essence of earthquake engineering, including in particular the seismic isolation concept, is basically to achieve an acceptable compromise for the structure displacements (stiffness) and stresses/strains (resistance) relation.

The adopted large foundation corresponds to lower and stiffer real buildings where the rocking effect during an earthquake is small or negligible, while the small foundation corresponds to higher real buildings with lower ground plans and greater bending influence. The efficiency of the considered seismic isolation is expected to be lower (more conservative) for models with larger foundation than for models with smaller foundation. The present research was conducted to further determine the conservative efficiency of considered seismic isolation for the most unfavourable expected conditions and possible applications in practice.

6. Test results for one-time base accelerations ($a_{g,max}$=0.3 g for M_1 and M_2 and with $a_{g,max}$=0.2 g for M_3 and M_4)

6.1 Peak values of the measured quantities

The peak values of the measured quantities are presented on Figs. 4 - 7. $\varepsilon_{1,2}$ refers to a larger (less favourable) value of ε_1 and ε_2, whereas $v_{1,2}$ refers to a larger (less favourable) value of v_1 and v_2, respectively. It can be seen from Figs. 4 - 7 that the effect of the size of the foundation on the peak values of a, $\varepsilon_{1,2}$, $u_{1,2}$, $v_{1,2}$ depends on the stiffness of the model (M_1, M_2, M_3 and M_4), the type of excitation (AA, AP, AS, ABL) and the type of substrate (RB, BI).

Authors are aware that there is a lot of data and variables in the manuscript. Unfortunately, due to limited space, it is not possible to explain and comment on all the results in detail. By careful analysis of presented Figs. 4 - 7., it can be concluded that a larger foundation (LF), compared to a smaller foundation (SF) results in the following:

- Higher acceleration a for all models and all excitations. The exceptions where the M_3 and M_4

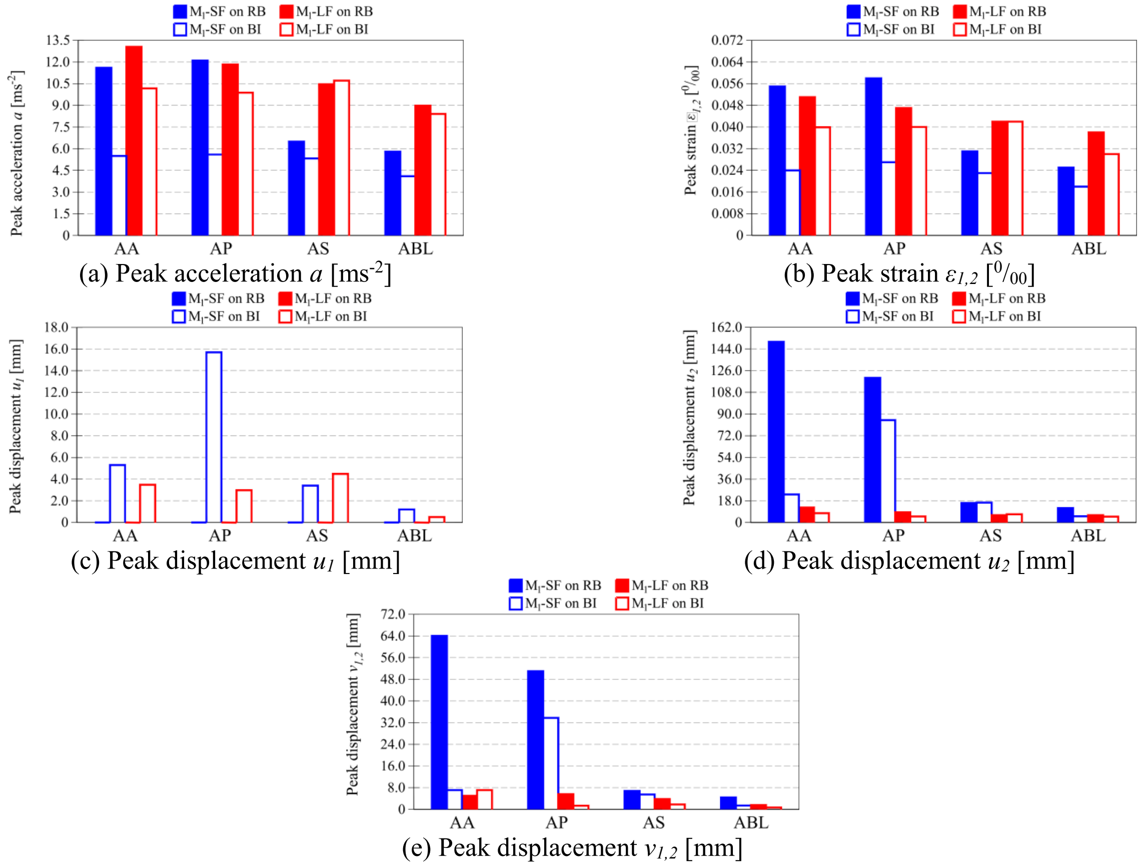

Fig. 4 Peak values of the results for the M_1 model

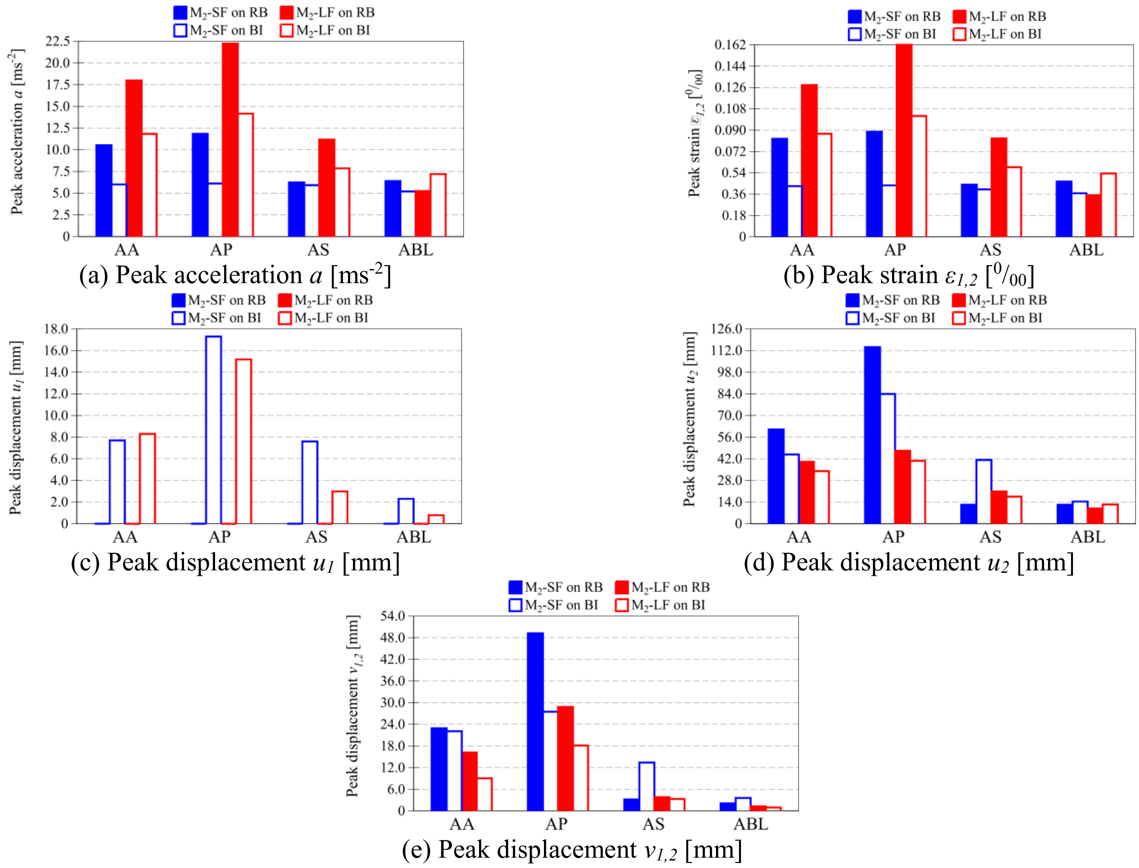

Fig. 5. Peak values of the results for the M_2 model

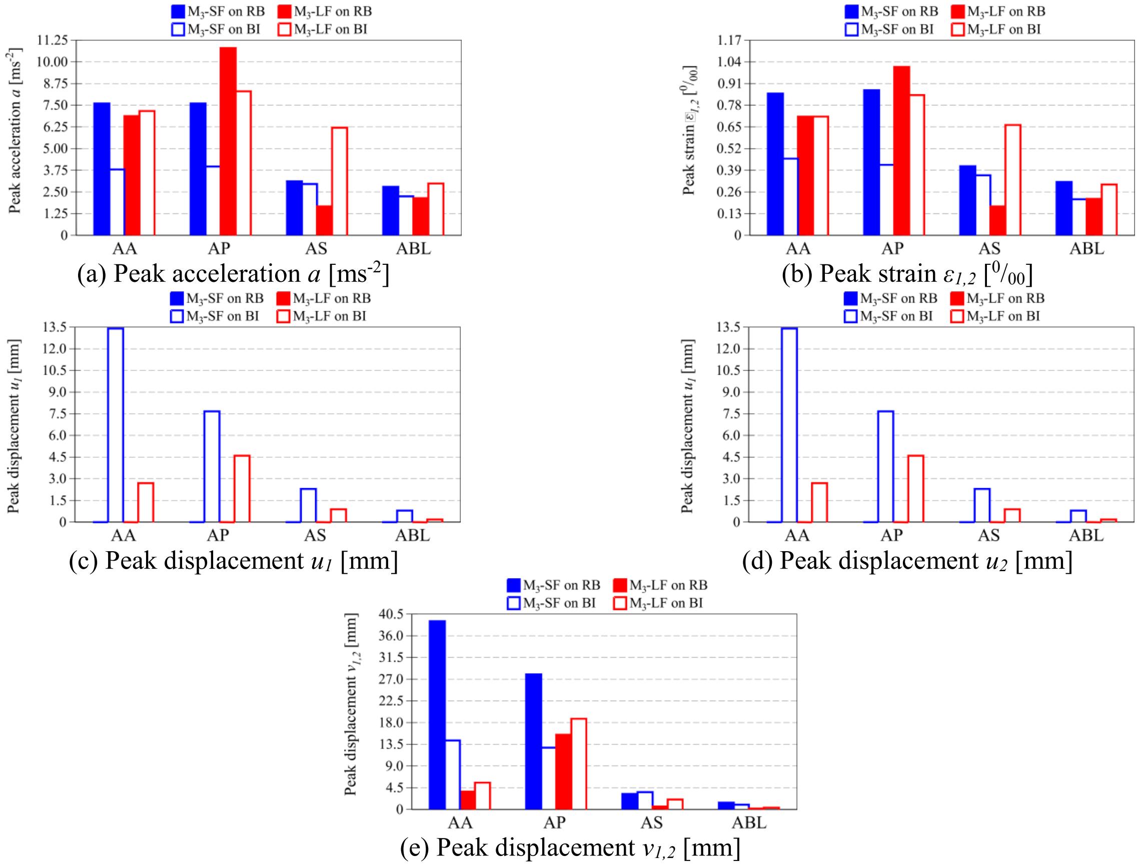

(a) Peak acceleration a [ms^{-2}] (b) Peak strain $\varepsilon_{1,2}$ [$^0/_{00}$]

(c) Peak displacement u_1 [mm] (d) Peak displacement u_2 [mm]

(e) Peak displacement $v_{1,2}$ [mm]

Fig. 6 Peak values of the results for the M_3 model

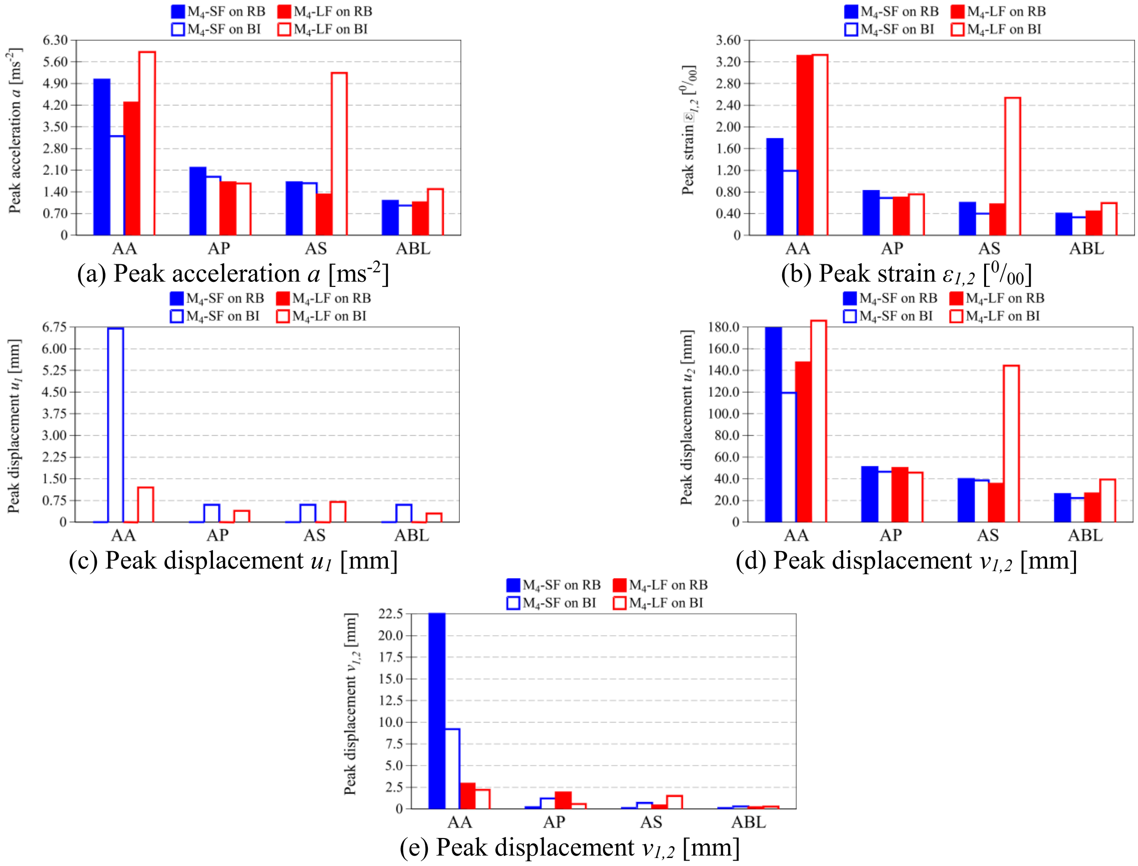

(a) Peak acceleration a [ms^{-2}] (b) Peak strain $\varepsilon_{1,2}$ [$^0/_{00}$]

(c) Peak displacement u_1 [mm] (d) Peak displacement $v_{1,2}$ [mm]

(e) Peak displacement $v_{1,2}$ [mm]

Fig. 7 Peak values of the results for the M_4 model models based on RB. Higher accelerations may not always result in greater displacements and strains.

- Predominantly larger strains $\varepsilon_{1,2}$ were obtained for model M_4 at AA and AS excitations. For AA excitation, steel yielding at the bottom of the column occurred (the start of the plastic deformation for steel S355 occurred at 1.7 $^0/_{00}$).
- Significantly smaller displacements u_1 were obtained for almost all the models and excitations.
- Significantly smaller u_2 displacements were obtained for almost all the models and excitations. The larger displacements were only found for model M_4 at AA and AS excitations, where steel yielding at the bottom of the column occurred.
- Significantly smaller vertical displacements of foundation $v_{1,2}$ for almost all models and excitations.

The increased layout size of the foundation results in an increased rotational stiffness and reduced foundation rotation angle. Thus, the effect of rocking decreases and indirectly increases the rigidity of the model. This results in slightly higher earthquake accelerations (forces) but smaller horizontal and vertical displacements. Additionally, strains at the bottom of the column increase, especially for the M_4 model with the lowest stiffness. For this model, a larger foundation significantly contributes to the increase in the column restraint in the base.

The AA and AP excitations were generally significantly less favourable than the AS and ABL excitations. The exception is the M_4 model, where the AS excitation was less favourable than the AP excitation.

One of the key indicators of the aseismic layer efficiency, relative to the rigid base, is the measured strains $\varepsilon_{1,2}$ at the bottom of the column. The analysis of Figs. 4-7. shows that $\varepsilon_{1,2}$ values for M_3 and M_4 models with a larger foundation (LF) are larger for the foundation on base isolation (BI) than for the foundation on rigid base (RB). This result confirms the assumption at the beginning of the study for the considered concept of seismic isolation that it is likely to be favourable only for very rigid and rigid lower structures based on stiff ground.

6.2 Time-history presentation of the results

Only some of the time histories of the measured quantities are presented in Figs. 8 - 15. The time histories are presented to show changes in the considered quantity depending on the model type, foundation size, earthquake type, and substrate type. Additionally, the results are presented for the purpose of possible numerical simulation the performed experimental tests.

Fig. 8 presents the vertical strain on the right bottom side of the steel column ε_1 for accelerogram AA. It can be seen that the smallest strains are recorded from the very stiff model M_1 and the largest strains are recorded from the soft model M_4. Additionally, for the M_4 model, there was an increase in the strain for the large foundation (LF) with base isolation (BI), compared to that of small foundation (SF) with base isolation (BI) and a significant plastic (irreversible) strain.

Fig. 9 presents the horizontal displacement of the mass

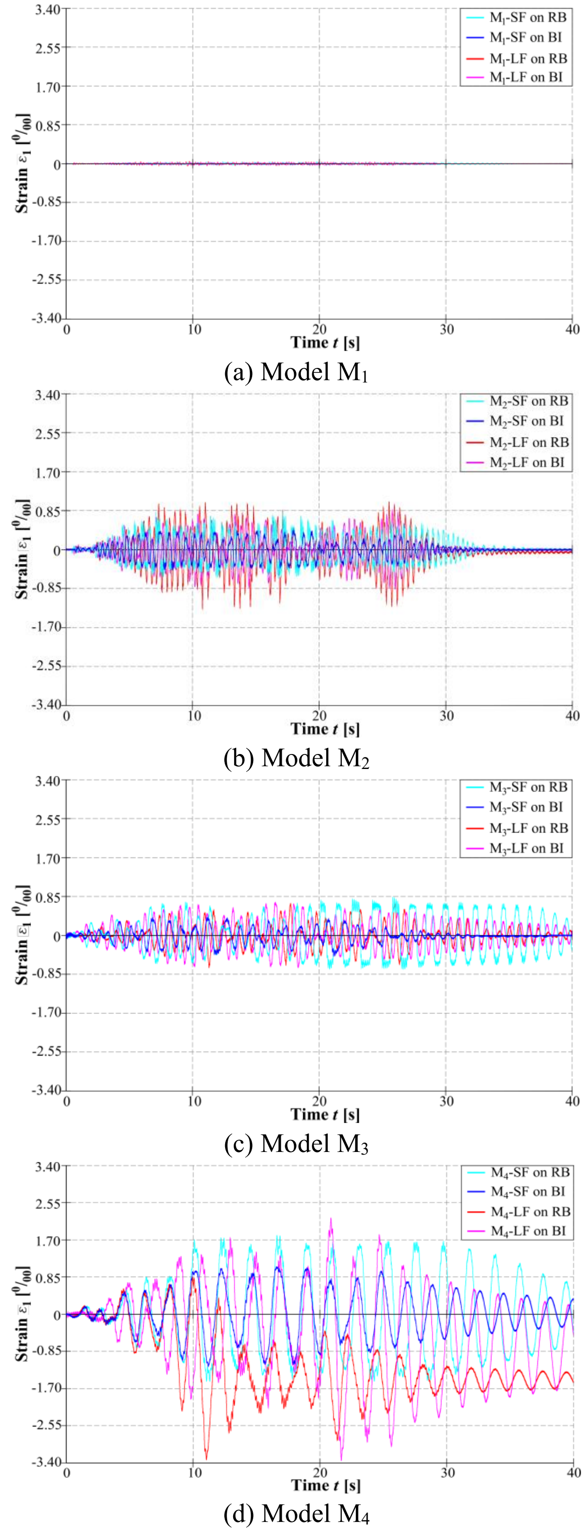

Fig. 8 Vertical strain on the right bottom side of the steel column ε_1 for accelerogram AA

centre at the column top u_2 for accelerogram AA. The displacements are largest for the softer models (M_3 and M_4). For models M_1, M_2, and M_3 with a larger foundation (LF), the displacements are significantly smaller than those for the models with a small foundation (SF), and the displacements are elastic (reversible). For M_4 with a large

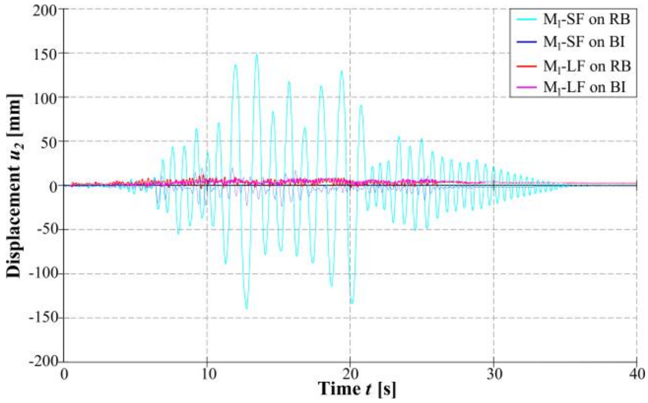

(a) Model M$_1$

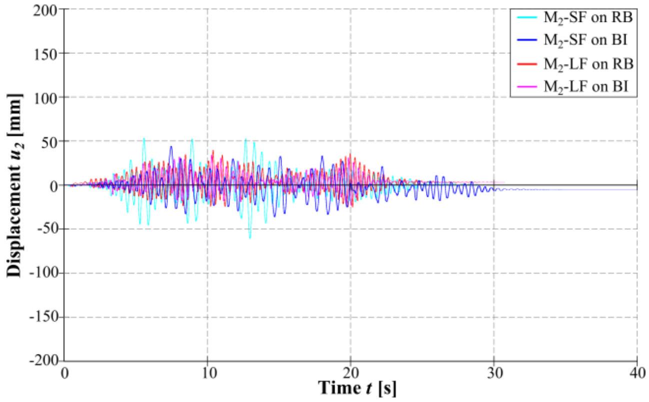

(b) Model M$_2$

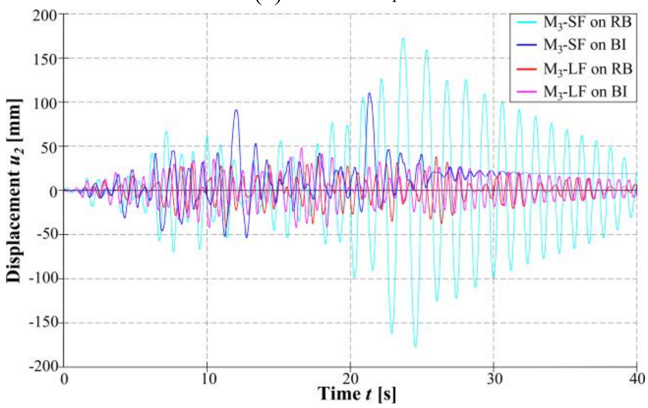

(c) Model M$_3$

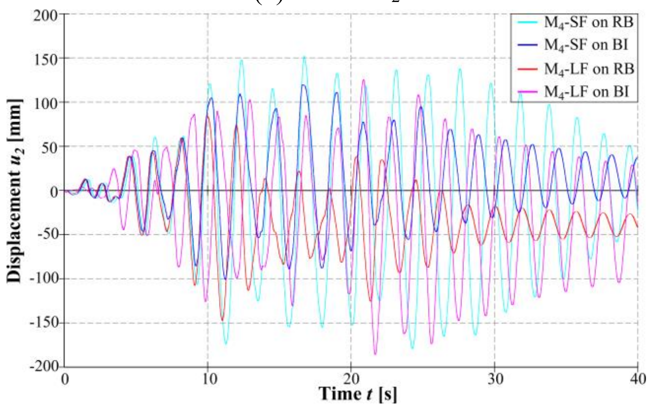

(d) Model M$_4$

Fig. 9 Horizontal displacement of the mass centre at the column top u_2 for accelerogram AA

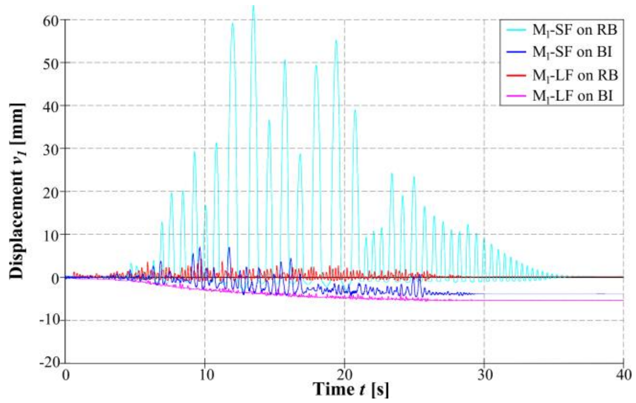

(a) Model M$_1$

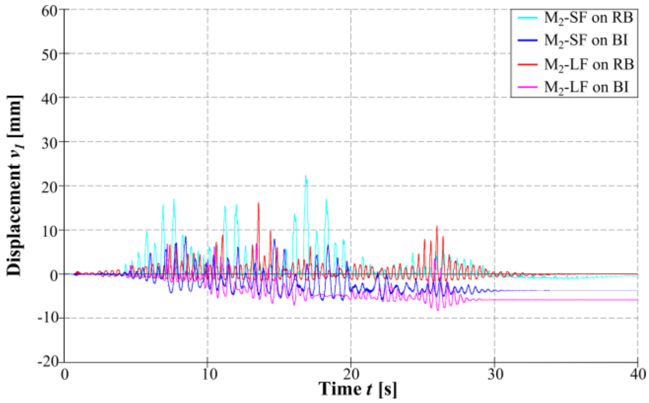

(b) Model M$_2$

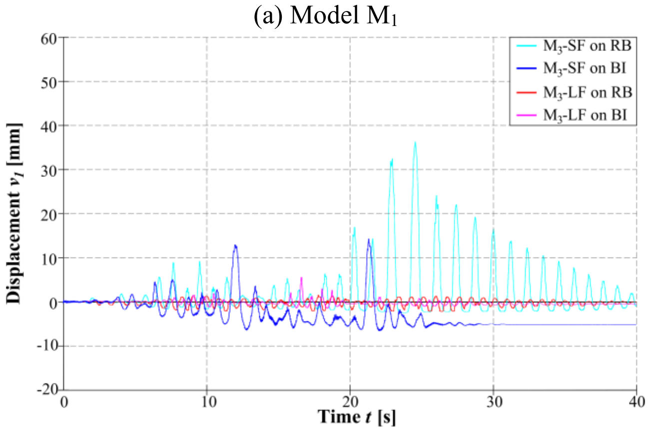

(c) Model M$_3$

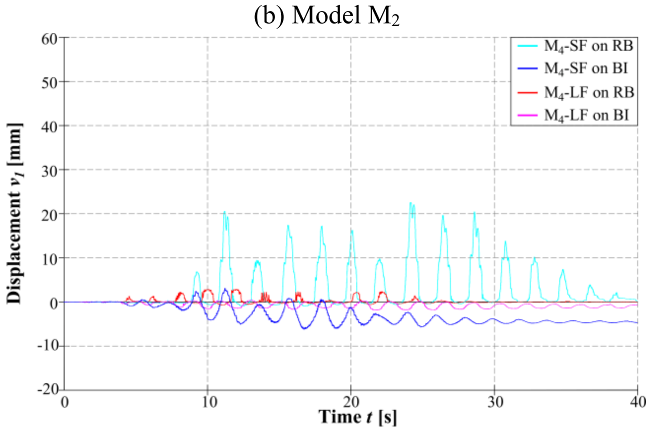

(d) Model M$_4$

Fig. 10 Vertical displacement at the left edge of the foundation v_1 for accelerogram AA

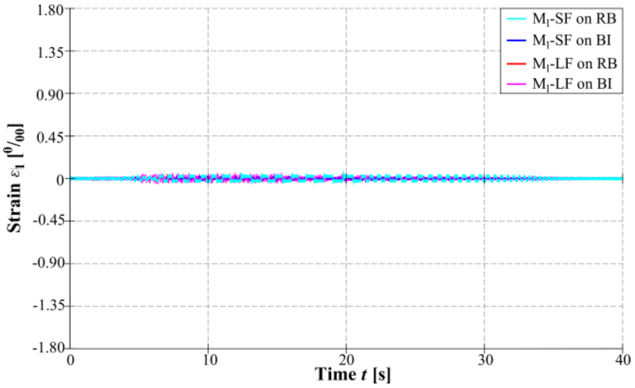

(a) Model M_1

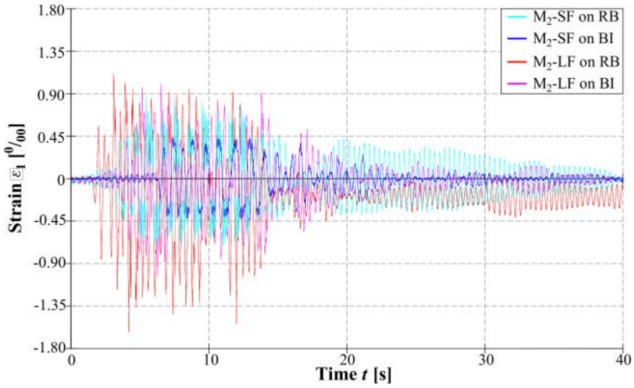

(b) Model M_2

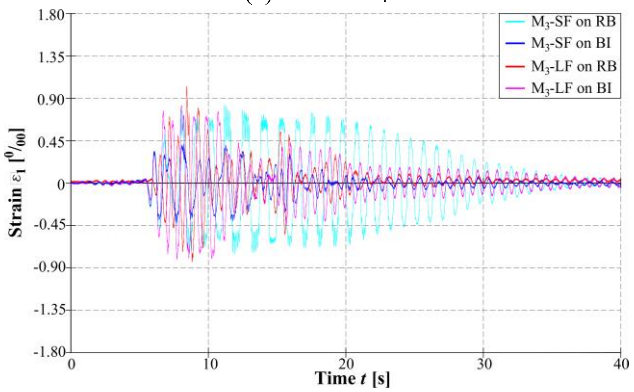

(c) Model M_3

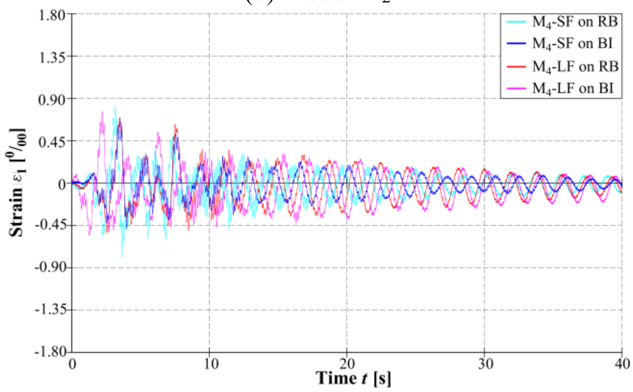

(d) Model M_4

Fig. 11 Vertical strain on the right bottom side of the steel column ε_1 for accelerogram AP

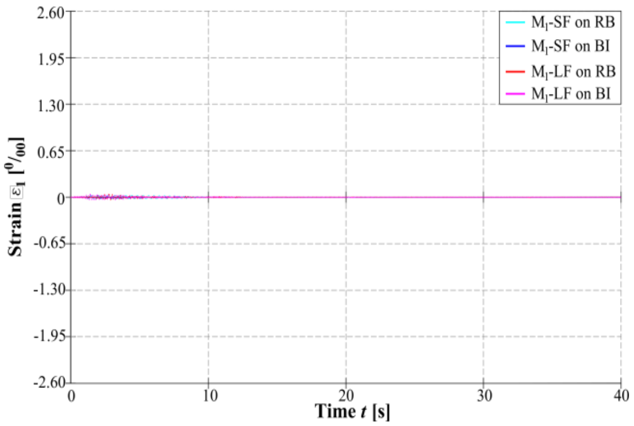

(a) Model M_1

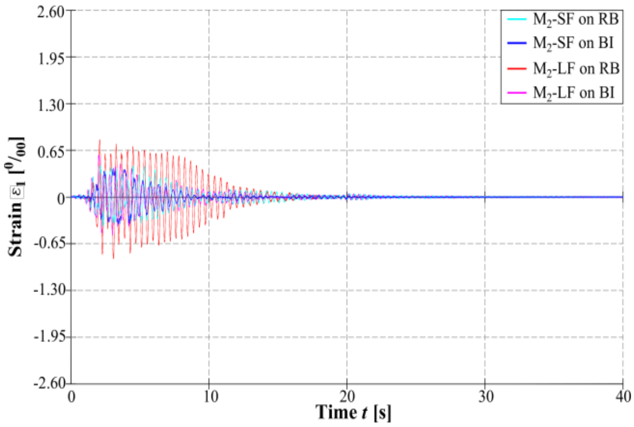

(b) Model M_2

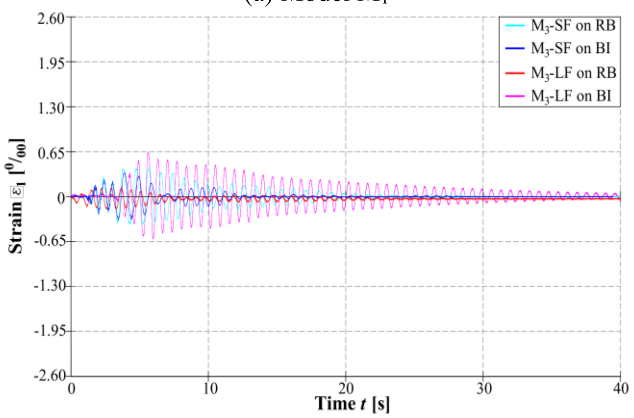

(c) Model M_3

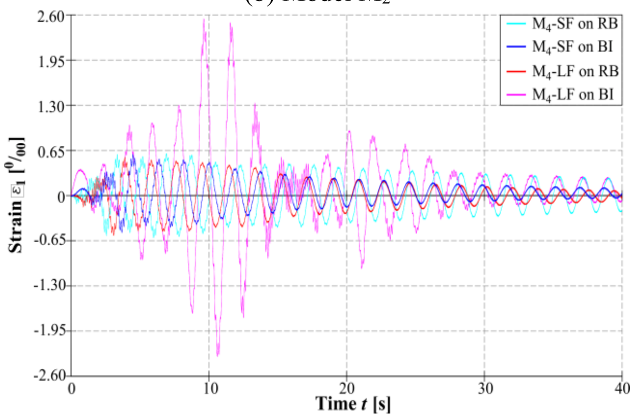

(d) Model M_4

Fig. 12 Vertical strain on the right bottom side of the steel column ε_1 for accelerogram AS

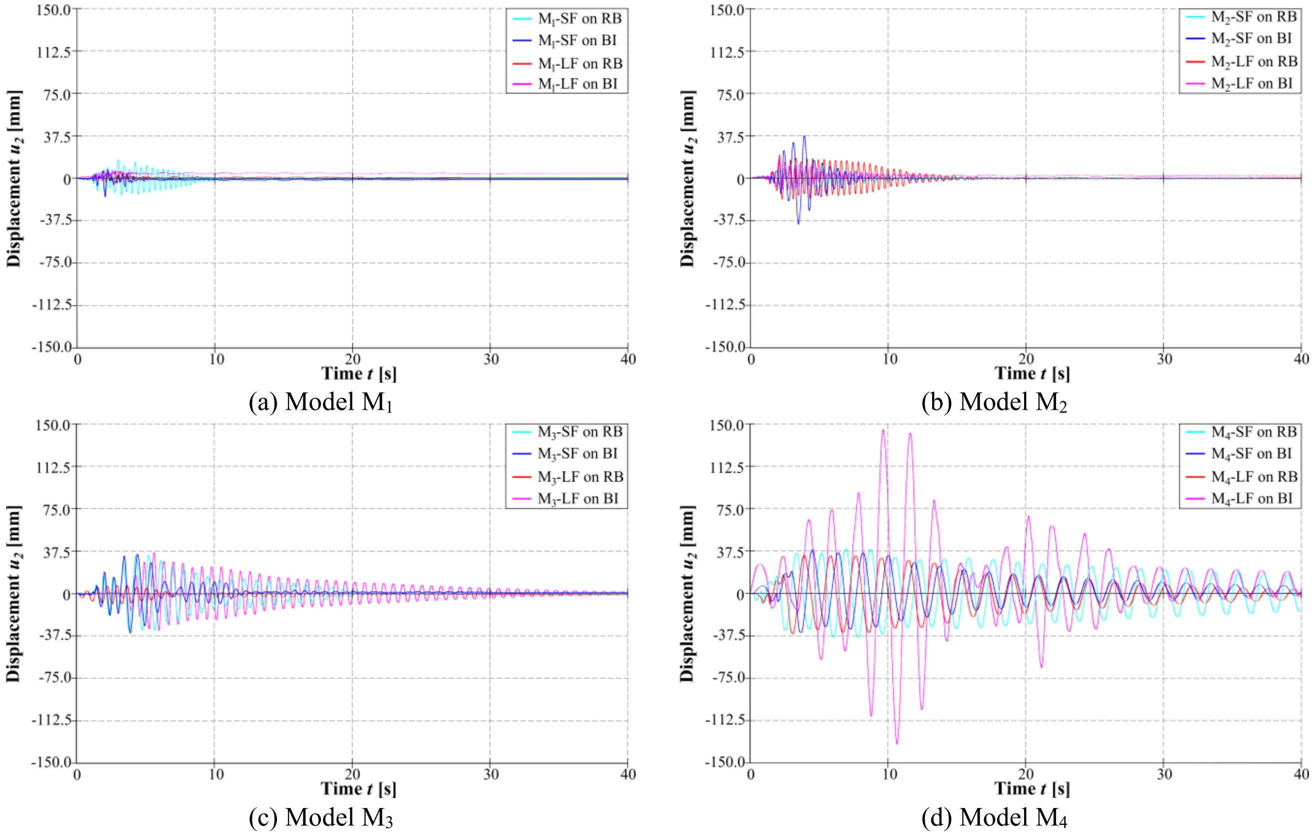

(a) Model M_1 (b) Model M_2

(c) Model M_3 (d) Model M_4

Fig. 13 Horizontal displacement of the mass centre at the column top u_2 for accelerogram AS

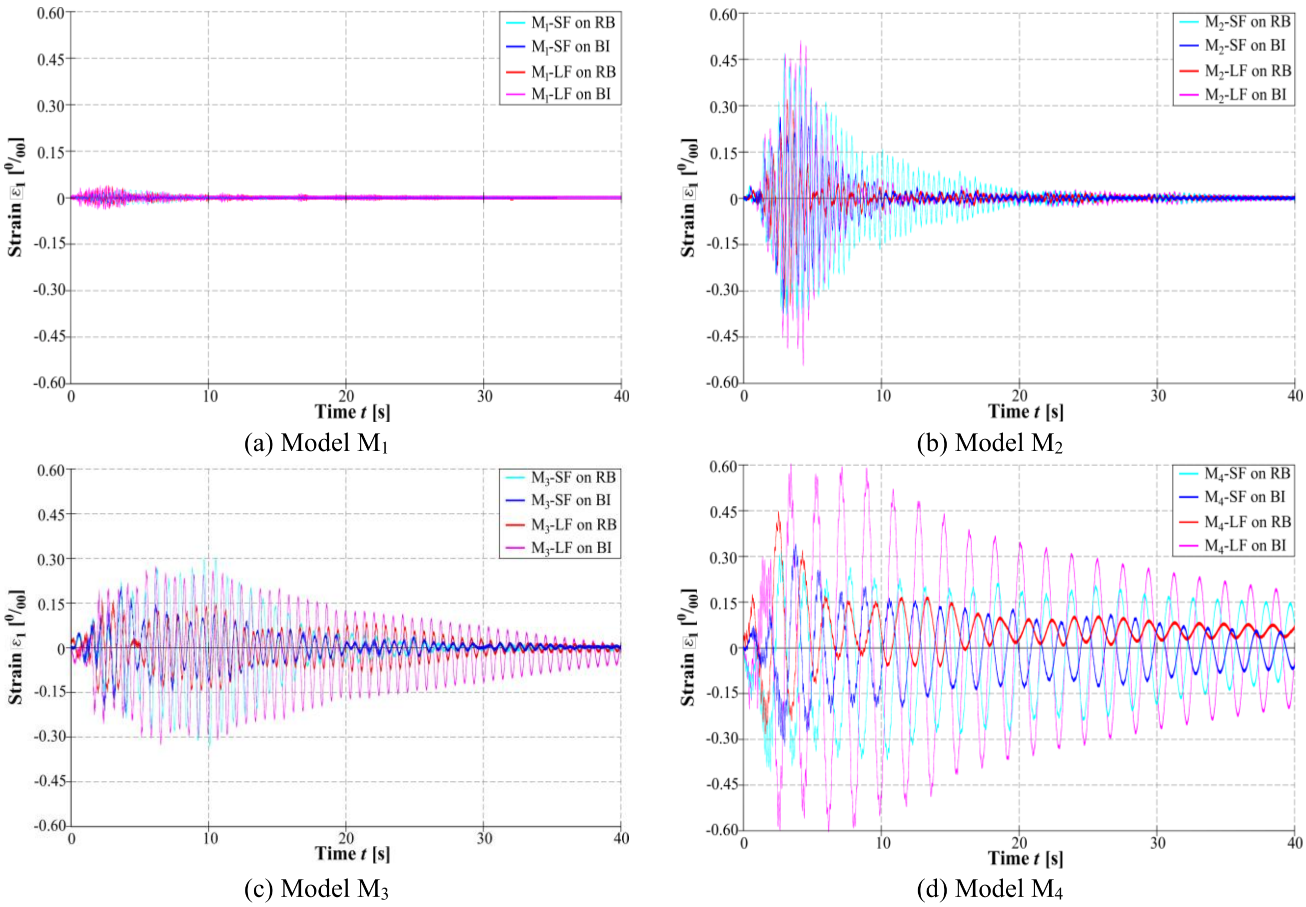

(a) Model M_1 (b) Model M_2

(c) Model M_3 (d) Model M_4

Fig. 14 Vertical strain on the right bottom side of the steel column ε_1 for accelerogram ABL

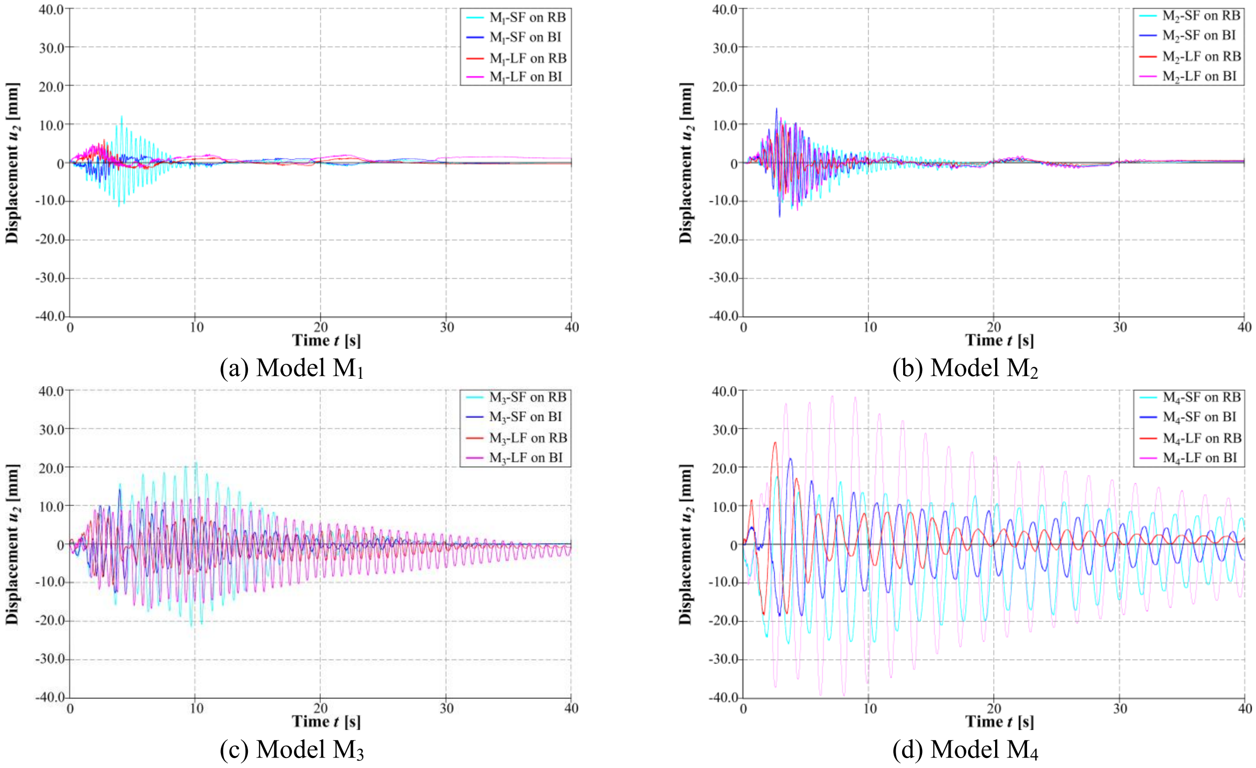

Fig. 15 Horizontal displacement of the mass centre at the column top u_2 for accelerogram ABL

Table 1 Coefficients of seismic isolation efficiency

Coefficient	Excitation	Model							
		M_1		M_2		M_3		M_4	
		M_1-SF	M_1-LF	M_2-SF	M_2-LF	M_3-SF	M_3-LF	M_4-SF	M_4-LF
c_a	AA	0.47	0.78	0.57	0.68	0.50	1.04	0.64	1.38
	AP	0.46	0.84	0.52	0.64	0.52	0.77	0.87	0.98
	AS	0.82	1.03	0.95	0.66	0.83	3.72	0.98	3.98
	ABL	0.71	0.94	0.81	1.38	0.80	1.40	0.86	1.41
$c_{\varepsilon 1,2}$	AA	0.44	0.78	0.52	0.68	0.54	1.00	0.67	1.01
	AP	0.47	0.85	0.49	0.63	0.49	0.84	0.84	1.09
	AS	0.74	1.00	0.91	0.71	0.87	3.83	1.00	4.44
	ABL	0.72	0.89	0.79	1.53	0.68	1.39	0.85	1.37
c_{u2}	AA	0.16	0.64	0.73	0.85	0.62	1.16	0.67	1.26
	AP	0.71	0.61	0.73	0.87	0.57	0.99	0.92	0.92
	AS	1.02	1.16	3.38	0.85	0.92	3.88	0.97	4.10
	ABL	0.43	0.82	1.18	1.27	0.68	1.39	0.86	1.49
$c_{v1,2}$	AA	0.11	1.44	0.96	0.56	0.37	1.51	0.41	0.75
	AP	0.66	0.30	0.56	0.63	0.46	1.21	5.26	0.30
	AS	0.81	0.49	4.16	0.89	1.13	3.45	5.23	4.03
	ABL	0.66	0.30	0.56	0.63	0.46	1.21	2.89	1.48

foundation (LF), compared to the small foundation (SF), the displacements are larger and irreversible.

Comparing Figs. 11 and 8, it can be concluded that for models M_1, M_2 and M_3, the strain ε_1 is approximately the same for AA and AP excitations. The authors explain this behaviour that probably AA led to the resonant motion of the M_4 model. Namely, the AA excitation contains a wide range of frequencies and is often the most unfavourable excitation. It should be noted that the excitation AP also causes high strains in the model M_4.

The vertical strain on the right bottom side of steel column ε_1 for accelerogram AS (Fig. 12) has higher values for all models with a large foundation (LF), particularly for the M_4 model, compared to values for models with a small foundation.

The horizontal displacement of the mass centre at the column top u_2 for accelerogram AS (Fig. 13), compared to the SF case, is slightly smaller for the LF case for models M_1, M_2, and M_3 and significantly larger for model M_4. All the displacements are reversible.

For the ABL excitation, the vertical strain ε_1 (Fig. 14) and the horizontal displacement u_2 (Fig. 15) are also largest for the M_4 model, with a LF resulting in a significantly larger ε_1 and u_2 than those with a SF. For the other models, the values of these quantities are approximately equal for the LF and SF models.

6.3 Seismic isolation efficiency

Table 1 presents the efficiency of the considered seismic isolation for one-time base excitation ($a_{g,max}$=0.3 g for M_1 and M_2 and with $a_{g,max}$=0.2 g for M_3 and M_4), depending on the model type, foundation size, earthquake type, and substrate type. The seismic isolation efficiency coefficients c_a, $c_{\varepsilon1,2}$, c_{u2} and $c_{v1,2}$ are defined as the ratio of the highest value of the considered model parameter (acceleration, strain, displacement) on the aseismic layer (h_p=0.3 m) and the model supported on a rigid base. The $c_{\varepsilon1,2}$ and $c_{v1,2}$ tags refer to the larger values of ε_1 and ε_2 (v_1 and v_2), respectively. Thus, if the coefficients are less than 1.0, the corresponding parameters are smaller (more favourable) for the pebble layer (BI)-based models than for the rigid base (RB)-based models. Otherwise, the corresponding parameters are higher (less favourable) for the BI-based models (values in the rectangle in Table 1) than for the other models.

When evaluating the importance of the considered coefficients, it should be noted that the accelerograms of the longer duration and longer predominant period AA and AP give significantly higher strains (stresses) and displacements than those of the short period, impact AS and ABL accelerograms. Namely, these coefficients represent relative relationships, regardless of the level of strain and displacement for each excitation. Further, irrespective on the foundation size and structural stiffness, seismic isolation efficiency was higher for AA and AP excitation than for AS and ABL. This behaviour is explained by the fact that AA and AP are long-lasting earthquakes that bring high energy into the system and produce more pronounced rocking of the model. Namely, beside the sliding mechanism, the reduction or earthquake forces in this isolation concept is achieved by reduced rocking stiffness, taking the advantages of rocking isolation concept.

The most important coefficients are those related to the strains (stresses) at the bottom of the column and to the displacements. Higher model accelerations do not necessarily result in larger strains; therefore the strain coefficient more accurately describes the real state in the structure than the acceleration coefficient.

The larger foundation (LF) models generally have a less favourable strain state and a more favourable displacement state than those of the small foundation (SF) models. It is also evident that with decreasing stiffness in the model (increasing its period of free oscillations), the efficiency of the considered seismic isolation decreases. For example, the ratio of the coefficient $c_{\varepsilon1,2}$ for models with a larger foundation, namely, M_1-LF, M_2-LF, M_3-LF, and M_4-LF are 0.78, 0.68, 1.00, and 1.01 for excitation AA; 0.85, 0.63, 0.84, and 1.09 for excitation AS; 0.85, 0.63, 0.84, and 1.09 for excitation AP; and 0.89, 1.53, 1.39, and 1.37 for ABL excitation. Thus, even for the most conservative case of a building with virtually no foundation rotation, the considered seismic isolation with earthquake stresses in the elastic region results in a significant reduction of the strains (stresses) in the construction of very stiff (M_1) and stiff (M_2) buildings but also somewhat reduce the strains for softer buildings (M_3 and M_4) for some earthquake loading conditions.

The ratio of the coefficients c_{u2} for the models M_1-LF, M_2-LF, M_3-LF, and M_4-LF are 0.64, 0.85, 1.16, and 1.26 for the AA excitation; 0.61, 0.87, 0.99, and 0.92 for the AP excitation; 1.16, 0.85, 3.88, and 4.10 for the AS excitation; and 0.82, 1.27, 1.39, and 1.49 for the ABL excitation. Thus, the presented seismic base isolation is also favourable in terms of the horizontal displacements for the M_1 and M_2 models. As seen in Figs. 6 and 7., the impact accelerogram of AS excitation is proven to be very unfavourable for softer models M_3 and M_4 with a large foundation, which can be explained by the large influence of the shear force.

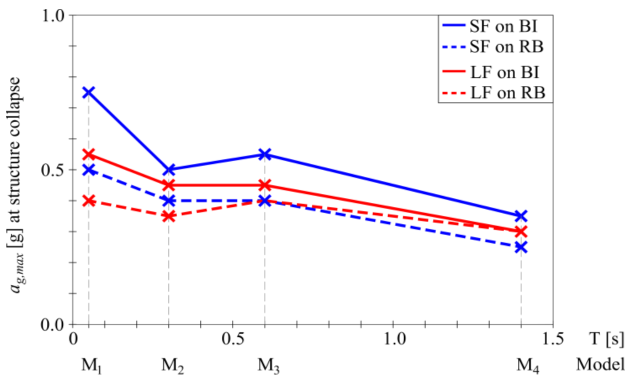

Fig. 16 Acceleration $a_{g,\,max}$ [g] of accelerogram AA at which the structure collapsed

7. Test results for a successive increase in the base acceleration until structure collapsed

The acceleration $a_{g,\,max}$ for AA excitation (mainly the most unfavourable excitation) at which the tested model collapsed or lost stability, is shown in Fig. 16.

The purpose of this test was to determine how much the bearing capacity of the model supported by the 0.3 m thick aseismic layer exceeds the bearing capacity of the same model supported by a rigid base, separately for the small foundation (SF) case and large foundation (LF) case. The ratios (coefficients) for models with a small foundation (SF) for M_1-SF, M_2-SF, M_3-SF, and M_4-SF were 1.50, 1.25, 1.38, and 1.40, and for models with a large foundation (LF) for M_1-LF, M_2-LF, M_3-LF, and M_4-LF were 1.38, 1.29, 1.19, and 1.00. The accuracy of the results on Fig. 16 would be higher if $\Delta a_{g,\,max}$ was less than 0.05 g. From the above results, it can be concluded that with the increase in the ground dimensions of the foundation, the limit state efficiency of the considered seismic isolation decreases. Additionally, it can be noted that as the period of free oscillations of the model increases (decrease in stiffness), the limit state efficiency of the considered seismic isolation decreases. Thus, the ratio of acceleration $a_{g,\ max}$ at which the model collapsed for seismic isolation (BI) and $a_{g,\ max}$ at which the model collapsed for a rigid base (RB) for the M_3-LF medium-stiff model is 1.13, and for the M_4-LF soft model, the ratio is only 1.0.

8. Conclusions

The following conclusions can be made based on the research results of the effect of the ground plan dimension of the foundation on the seismic base isolation efficiency using a layer of stone pebbles for building models with four different stiffnesses (from very rigid M_1 to soft M_4) exposed to the acceleration of four different types of earthquakes (AA and AP of longer duration and longer predominant period, and AS and ABL with short duration and impact type).

For the case of the one-time base acceleration of the adopted excitations with $a_{g,\ max}$=0.2 g (M_1 and M_2 model) or $a_{g,\ max}$=0.2 g (M_3 and M_4 model), which causes only elastic strains/stresses in the model column (except for the M_4 model at AA excitation), the following general conclusions apply:

- Compared to models with smaller foundations, models with larger foundations result in higher accelerations, larger column strains (especially for the soft M_4 model), significantly smaller foundation and column top displacements, and significantly smaller vertical foundation displacements (settlement and uplifting).
- The reason for the foregoing is a significant increase in rotational stiffness at a larger foundation and a decrease in the foundation rotation, i.e., a decrease in the effect of rocking. This results in an indirect increase in the stiffness of the entire model and the generation of higher earthquake accelerations (forces) in the model.
- As the size of the foundation increases, the efficiency of the seismic base isolation with the layer of stone pebbles decreases. The seismic isolation efficiency coefficient is defined as the ratio of the highest value of the considered quantity for the model parameter on the aseismic layer and for the model supported by a rigid base. Thus, the ratio of the coefficient of strain (stress) at the bottom of column $c_{\varepsilon 1,2}$ for models with larger foundations, namely, M_1-LF, M_2-LF, M_3-LF, and M_4-LF were 0.78, 0.68, 1.00, and 1.01 for excitation AA, 0.85, 0.63, 0.84, and 1.09 for excitation AS; 0.85, 0.63, 0.84, and 1.09 for excitation AP; and 0.89, 1.53, 1.39, and 1.37 for excitation ABL. Thus, even for the most unfavourable condition with very little foundation rotation, the considered seismic isolation results in a significant reduction in the strains at the bottom of the column in very stiff (M_1) and stiff (M_2) building models. The ratio of the displacement coefficients of the column top c_{u2} for models with a larger foundation for M_1-LF, M_2-LF, M_3-LF, and M_4-LF are 0.64, 0.85, 1.16, and 1.26 for the AA excitation; 0.61, 0.87, 0.99, and 0.92 for the AP excitation; 1.16, 0.85, 3.88, and 4.10 for the AS excitation; and 0.82, 1.27, 1.39, and 1.49 for the ABL excitation. It follows that the considered seismic base isolation also results in a smaller column top displacement u_2 for all the models subjected to AA and AP excitations. It can be concluded that the seismic base isolation has proven to be sufficiently effective for models of very stiff (M_1) and stiff (M_2) buildings with all the accelerograms applied.
- The difference in response of investigated models under accelerograms with long predominant periods (AA, AP) and the ones with short predominant periods (AS, ABL) is observed. Irrespective on the foundation size and structural stiffness, seismic isolation efficiency was higher for AA and AP excitation than for AS and ABL. This behaviour is explained by the fact that AA and AP are long-lasting earthquakes that bring high energy into the system and produce more pronounced rocking of the model. Namely, beside the sliding mechanism, the reduction or earthquake forces in this isolation concept is achieved by reduced rocking stiffness, taking the advantages of rocking isolation concept. The low efficiency of seismic isolation for AS and ABL accelerograms should be seen in the context that they cause low stresses in the tested models, which diminishes the fact of less efficient seismic isolation for such excitations.

Every model was exposed to a set of repeated artificial accelerogram (AA) (the most unfavourable excitation) by scaling the peak ground acceleration (PGA) until the structure collapsed or lost stability. The ratios of the acceleration $a_{g,max}$ (load-bearing capacity) of the considered models for the foundation supported on the stone pebble layer and the foundation supported on a rigid base for the small foundation case (SF) for M_1-SF, M_2-SF, M_3-SF, and M_4-SF were 1.50, 1.25, 1.38, and 1.40, and for the large foundation (LF) case, for M_1-LF, M_2-LF, M_3-LF, and M_4-LF the ratios were 1.38, 1.29, 1.13, and 1.00. Obviously, as the size of the foundation increases, the limit state efficiency of the seismic isolation decreases when reaching the model load-bearing capacity or losing stability. Additionally, reducing the stiffness of the model (the column), with the same foundation, reduces the limit state efficiency of the seismic isolation. Thus, the ratio of the acceleration $a_{g,\ max}$ at which the model collapses for seismic isolation and $a_{g,\ max}$ at which the model collapses for a rigid base for the M_3-LF medium-stiff model is 1.13, and for the M_4-LF soft model is only 1.0. Therefore, the research carried out to the collapse condition of the considered models confirms that the seismic isolation limit state efficiency decreases with the increase in the model foundation and with the decrease in the column stiffness. However, for very stiff (M_1) and stiff (M_2) models supported on the large foundation with low rocking effect, seismic isolation with a thin layer of stone pebbles can significantly increase load-bearing capacity of models (up to approximately 38%), depending on the type of earthquake.

The conducted research has confirmed the conclusions of the previous studies (Banović *et al*. 2018b, 2019) on the efficiency of the considered seismic isolation, which with new studies is reduced and restricted mainly to very stiff and stiff buildings on stiff soil (with a free oscillation period up to approximately 0.3 s - 0.4 s). Owing the limitations of the performed research (relative simple building models, just four building models, only four base excitations applied, and uniaxial base excitation), the obtained conclusions should be strengthened by further research. Due to the above statement, further experimental research on this topic (preferably on real structures or models with realistic material and a slightly reduced geometry) and research using numerical models are needed.

Acknowledgments

This work has been fully supported by the Croatian Science Foundation under the project *"Seismic base isolation of a building by using natural materials - shake table testing and numerical modelling*" [IP-06-2016-5325]. The work of doctoral student Ivan Banović has been fully supported by the *"Young researchers' career development project – training of doctoral students"* of the Croatian Science Foundation funded by the European Union from the European Social Fund. The authors are grateful for the support.

References

Ambraseys, N., Smit, P., Sigbjornsson, R., Suhadolc, P. and Margaris, M. (2001), EVR1-CT-1999-40008, European Commission, Directorate-General XII, Environmental and Climate Programme, Brussels, Belgium

Anastasopoulos, I., Loli, M., Georgarakos, T. and Drosos, V. (2012), "Shaking table testing of rocking-isolated bridge pier on sand", *J. Earthq. Eng.*, **17**(1), 1-32. https://doi.org/10.1016/j.soildyn.2012.04.006.

Azinović, B., Kilar, V. and Koren, D. (2014), "The seismic response of low-energy buildings founded on a thermal insulation layer –a parametric study", *Eng. Struct.*, **81**, 398-411. https://doi.org/10.1016/j.engstruct.2014.10.015.

Azinović, B., Kilar, V. and Koren, D. (2016), "Energy-efficient solution for the foundation of passive houses in earthquake-prone regions", *Eng. Struct.*, **112**, 133-145. https://doi.org/10.1016/j.engstruct.2016.01.015.

Azzam, W., Ayeldeen, M. and El Siragy, M. (2018), "Improving the structural stability during earthquakes using in-filled trench with EPS geofoam—numerical study", *Arab. J. Geosci.*, **11**(14), 395. https://doi.org/10.1007/s12517-018-3739-4.

Bandyopadhyay, S., Sengupta, A. and Reddy, G.R. (2015), "Performance of sand and shredded rubber tire mixture as a natural base isolator for earthquake protection", *Earthq. Eng. Eng. Vib.*, **14**(4), 683-693. https://doi.org/10.1007/s11803-015-0053-y.

Banović, I., Radnić, J. and Grgić, N. (2018b), "Shake table study on the efficiency of seismic base isolation using natural stone pebbles", *Advan. Mater. Sci. Eng.*, 1012527, https://doi.org/10.1155/2018/1012527.

Banović, I., Radnić, J. and Grgić, N. (2019), "Geotechnical seismic isolation system based on sliding mechanism using stone pebble layer: shake-table experiments", *Shock Vib.*, 9346232, https://doi.org/10.1155/2019/9346232.

Banović, I., Radnić, J., Grgić, N. and Matešan, D. (2018a), "The use of limestone sand for the seismic base isolation of structures", *Advan. Civil Eng.*, https://doi.org/10.1155/2018/9734283.

Brunet, S., de la Llera, J.C. and Kausel, E. (2016), "Non-linear modeling of seismic isolation systems made of recycled tire-rubber", *Soil Dyn. Earthq. Eng.*, **85**, 134-145. https://doi.org/10.1016/j.soildyn.2016.03.019.

Carpani, B. (2017). Base isolation from a historical perspective. 16th World Conference on Earthquake, Paper N° 4934, Santiago, Chile

Chung Y.L., Du L.J. and Pan H.H. (2019), "Performance evaluation of a rocking steel column base equipped with asymmetrical resistance friction damper", *Earthq. Struct.*, **17**(1), 49-61. https://doi.org/10.12989/eas.2019.17.1.049.

Doudoumis, I., Papadopoulos, P. and Papaliangas, T. (2002), "Low-cost base isolation system on artificial soil layers with low shearing resistance", Proceedings of the 12th European Conference on Earthquake Engineering, London, U.K.

Eurocode (2004) EN 1998-1:2004 Eurocode 8: Design of structures for earthquake resistance-Part 1: general rules, seismic actions and rules for buildings, European Committee for Standardization (CEN), Brussels, Belgium

Feng, R., Chen, Y. and Cui, G. (2018), "Dynamic response of post-tensioned rocking wall-moment frames under near-fault ground excitation", *Earthq. Struct.*, **15**(3), 243-251. https://doi.org/10.12989/eas.2018.15.3.243.

Forcellini, D. (2017), "Assessment on geotechnical seismic isolation (GSI) on bridge configurations", *Innovat. Infrastruct. Solution*., **2**(1), https://doi.org/10.1007/s41062-017-0057-8.

Hadad, H.A, Calabrese, A., Strano, S. and Serino, G. (2017), "A base isolation system for developing countries using discarded tyres filled with elastomeric recycled materials", *J. Earthq. Eng*., **21**(2), 246-266. https://doi.org/10.1080/13632469.2016.1172371.

Kalpakcı, V., Bonab, A.T., Özkan, M.Y. and Gülerce, Z. (2018), "Experimental evaluation of geomembrane/geotextile interface as base isolating system", *Geosynth. Int.*, **25**(1), 1-11. https://doi.org/10.1680/jgein.17.00025.

Karatzia, X. and Mylonakis, G. (2017), "Geotechnical seismic isolation using eps geofoam around piles", *The 6th International Conference on Computational Methods in Structural Dynamics and Earthquake Engineering*, Rhodes Island, Greece.

Koren, D. and Kilar, V. (2016), "Seismic vulnerability of reinforced concrete building structures founded on an XPS layer", *Earthq. Struct.*, **10**(4), 939-963. https://doi.org/10.12989/eas.2016.10.4.939.

Kulukčija S. and Humo M. (2009), "Survey of historic foundation engineering", Baština, Sarajevo.

Kulukčija S., Humo M., Mandžić E., Mandžić K., and Selimović M. (2009), "Existing historical foundation system of two old bridges from the Ottoman period in Bosnia and Herzegovina", *The Third International Congress on Construction History*, Cottbus, Germany.

Makris, N. (2014), "A half-century of rocking isolation", *Earthq. Struct.*, **7**(6), 1187-1221. https://doi.org/10.12989/eas.2014.7.6.1187.

Mavronicola, E., Komodromos, P. and Charmpis, D.C. (2010), "Numerical investigation of potential usage of rubber–soil mixtures as a distributed seismic isolation approach", *The Proceedings of the 10th International Conference on Computational Structures Technology*, Valencia, Spain.

Murillo, C., Thorel, L. and Caicedo, B. (2009), "Ground vibration isolation with geofoam barriers: centrifuge modelling", *Geotext. Geomembranes*, **27**(6), 423-434. https://doi.org/10.1016/j.geotexmem.2009.03.006.

Naeim, F. and Kelly, J.M. (1999), "Design of seismic isolated structures: From theory to practice", John Wiley & Sons, Inc., New York.

Nanda, R.P., Agarwal, P., and Shrikhande, M. (2012a), "Base isolation by geosynthetic for brick masonry buildings", *J. Vib.*

Control, **18**(6), 903-910. https://doi.org/10.1177/1077546311412411.

Nanda, R.P., Shrikhande, M. and Agarwal, P. (2012b), "Effect of ground motion characteristics on the pure friction isolation system", *Earthq. Struct.*, **3**(2), 169-180. https://doi.org/10.12989/eas.2012.3.2.169.

Panjamani, A., Devarahalli Ramegowda, M. and Divyesh, R. (2015), "Low cost damping scheme for low to medium rise buildings using rubber soil mixtures", *Japan. Geotech. Soc. Spec. Publications*, **3**(2), 24-28. https://doi.org/10.3208/jgssp.v03.i05.

Patil, S.J., Reddy, G.R., Shivshankar, R., Babu, R., Jayalekshmi, B.R. and Kumar, B. (2016), "Seismic base isolation for structures using river sand", *Earthq. Struct.*, **10**(4), 829-847. https://doi.org/10.12989/eas.2016.10.4.829.

Pecker, A. (2003), "A seismic foundation design process, lessons learned from two major projects: the Vasco de Gama and the Rion Antirion bridges", *The Proceedings of the ACI International Conference on Seismic Bridge Design and Retrofit*, La Jolla, U.S.A.

Pecker, A., Prevost, J.H. and Dormieux, L. (2001), "Analysis of pore pressure generation and dissipation in cohesionless materials during seismic loading", *J. Earthq. Eng.*, **5**(4), 441-464. https://doi.org/10.1080/13632460109350401.

Przewłócki, J., Dardzinska, I. and Swinianski, J. (2005), "Review of historical buildings' foundations", *Géotechnique*, **55**, 363-372. https://doi.org/10.1680/geot.2005.55.5.363.

Radnić, J., Grgić, N., Matešan, D. and Baloević, G. (2015), "Shake table testing of reinforced concrete columns with different layout size of foundation", *Materialwissenschaft und Werkstofftechnik*, **46**(4-5), 348-367. https://doi.org/10.1002/mawe.201500410.

Steenfelt, J.S, Foged, B. and Augustesen, A.H. (2015), "Izmit Bay bridge-geotechnical challenges and innovative solutions", *Int. J. Bridge Eng*., *(IJBE)* **3**(3), 53-68.

Tehrani, F.M. and Hasani, A. (1996), "Behaviour of Iranian low rise buildings on sliding base to earthquake excitation", *The Proceedings of the 11th World Conference on Earthquake Engineering*, Acapulco, Mexico.

Tsang, H.H. (2008), "Seismic isolation by rubber-soil mixtures for developing countries", *Earthq. Eng. Struct. Dyn.*, **37**(2), 283-303. https://doi.org/10.1002/eqe.756.

Tsang, H.H. (2009), "Geotechnical seismic isolation", *Earthq. Eng.: New Res., New York, U.S.A. Nova Science Publishers Inc.*, 55-87.

Tsang, H.H. and Pitilakis, K. (2019), "Mechanism of geotechnical seismic isolation system: analytical modeling", *Soil Dyn. Earthq. Eng.*, **122**, 171-184. https://doi.org/10.1016/j.soildyn.2019.03.037.

Tsang, H.H., Lo, S.H., Xu, X. and Neaz Sheikh, M. (2012), "Seismic isolation for low-to-medium-rise buildings using granulated rubber-soil mixtures: numerical study", *Earthq. Eng. Struct. Dyn.*, **41**(14), 2009-2024. https://doi.org/10.1002/eqe.2171.

Tsiavos, A., Alexander N.A., Diambra A., Ibraim E., Vardanega P. J., Gonzalez-Buelga A. and Sextos A. (2019), "A sand-rubber deformable granular layer as a low-cost seismic isolation strategy in developing countries: experimental investigation", *Soil Dyn. Earthq. Eng.*, **125** https://doi.org/10.1016/j.soildyn.2019.105731.

Wang J., He J.X., Yang Q.S. and Yang, N. (2018), "Study on mechanical behaviors of column foot joint in traditional timber structure", *Struct. Eng. Mech.*, **66**(1), 1-14. https://doi.org/10.12989/sem.2018.66.1.001.

Xiao, H., Butterworth, J.W. and Larkin, T. (2004), "Low-technology techniques for seismic isolation", *The Proceedings of the NZSEE Conference*, Rototua, New Zealand.

Xiong, W. and Li, Y. (2013), "Seismic isolation using granulated tire-soil mixtures for less-developed regions: experimental validation", *Earthq. Eng. Struct. Dyn.*, **42**(14), 2187-2193. https://doi.org/10.1002/eqe.2315.

Xiong, W., Yan, M.R., and Li, Y.Z. (2014), "Geotechnical seismic isolation system - further experimental study", *Appl. Mech. Mater.*, **580-583**, 1490-1493. https://doi.org/10.4028/www.scientific.net/AMM.580-583.1490.

Yegian, M. K. and Catan, M. (2004), "Soil isolation for seismic protection using a smooth synthetic liner", *J. Geotech. Geoenviron. Eng.*, **130**(11), 1131-1139. https://doi.org/10.1061/(ASCE)10900241(2004)130:11(1131).

Yegian, M.K. and Kadakal, U. (2004), "Foundation isolation for seismic protection using a smooth synthetic liner", *J. Geotech. Geoenviron. Eng.*, **130**(11), 1121-1130. https://doi.org/10.1061/(ASCE)10900241(2004)130:11(1121).

Zhao, X., Zhang, Q., Zhang, Q. and He, J. (2016), "Numerical study on seismic isolation effect of gravel cushion", *The Proceedings of the 7th International Conference on Discrete Element Methods*, **188**, 1055-1063., Dalian, China.

CC